

Precise Method for Measuring the Shear Surface Viscosity of Surfactant Monolayers

Jordan T. Petkov,* Krassimir D. Danov, and Nikolai D. Denkov

Laboratory of Thermodynamics and Physico-Chemical Hydrodynamics, Faculty of Chemistry, Sofia University, 1126 Sofia, Bulgaria

Richard Aust and Franz Durst

Lehrstuhl für Strömungsmechanik, Technische Fakultät, Friedrich-Alexander-Universität, Erlangen-Nürnberg, 91058 Erlangen, Germany

Received January 2, 1996[®]

A conceptually new and highly sensitive method for determining the shear surface viscosity of adsorbed or spread surfactant monolayers at a gas–liquid interface is presented. The surface viscosity is calculated from the drag coefficient of a small spherical particle floating at the interface under the action of an external capillary force. In this respect the method resembles the known Stokes method for measuring the bulk shear viscosity of liquids. The shear viscosity of adsorbed monolayers from sodium dodecyl sulfate and hexadecyltrimethylammonium bromide was measured. The sensitivity of the method is of the order of 10^{-8} Pa m s.

The shear surface viscosity of adsorbed monolayers of low molecular surfactants or polymers (including proteins) plays a crucial role in the dynamic processes at fluid interfaces. These are relevant to a variety of important technological problems like the formation, stability, and rheology of emulsions and foams, the industrial processes of film coating, spraying, flotation, oil recovery, etc.¹ as well as to some geophysical processes (e.g., air–sea interaction depends on dynamic monolayer characteristics²). For that reason several types of viscometers aimed at measuring the shear surface viscosity have been reported in the literature. The deep-channel viscometer³ is the most widely used one, due to its high sensitivity (of the order of 10^{-7} Pa m s) and relative simplicity. The basic shortcoming of the method is the need of tracer particles to visualize the interfacial velocity profile.⁴ The tracers are assumed to follow exactly the interfacial motion without disturbing it. A number of other specific problems with this method were discussed in the literature.⁴ A device avoiding these drawbacks is the disk surface viscometer. In this method the torsional stress on a rotating disk attached to a fluid interface^{5–8} is measured. The sensitivity of this kind of device is less than 10^{-5} Pa m s; hence they can be applied to systems of high interfacial viscosity (protein or other polymer layers). A similar class of viscometers based on torsional stress measurement is the knife-edge surface viscometers,^{9–11} which typically have the same sensitivity, 10^{-5} Pa m s. Only in the

rotating wall knife-edge viscometer^{12,13} a much higher sensitivity is achieved (of the order of 10^{-8} Pa m s) thanks to the usage of a small tracer particle, which is placed within the fluid interface to discern the interfacial rotational speed. Therefore, the existing methods are either of low sensitivity or need tracer particles, which could disturb the moving interface and compromise the measurement. As a result, the values reported in the literature for the interfacial shear viscosity of monolayers (especially of low molecular surfactants) are broadly scattered and sometimes differ by orders of magnitude for the same substance.^{13–15}

We propose a conceptually new method, in which the drag coefficient of a submillimeter-sized sphere floating on the interface is measured. We should note that *in our method the particle is not used as a tracer*. Instead, the sphere is set in motion under the action of an external force of known magnitude. The viscosity of the surfactant monolayer is determined through the particle drag coefficient. The force in our experiments arises from the lateral capillary interaction between the particle and a vertical plate^{16–18}—see Figure 1. In a vicinity of the plate the air–water interface is not perfectly flat (a curved meniscus is formed). Its shape can be determined solving the Laplace equation of capillarity at the respective boundary conditions. When the configuration shown in Figure 1 is realized, an attractive capillary force appears whose magnitude can be precisely calculated.¹⁶ When the particle–wall separation is large compared to the particle diameter, the capillary force is given by the following asymptotic expression

* To whom correspondence should be addressed: e-mail address, Jordan.Petkov@Ltph.cit.bg or jp@Ltph.chem.uni-sofia.bg.

[®] Abstract published in *Advance ACS Abstracts*, May 1, 1996.

(1) Malhotra, A. K.; Wasan, D. T. In *Thin Liquid Films: Fundamentals and Applications*; Ivanov, I. B., Ed.; Surfactant Science Series 29; Marcel Dekker, Inc.: New York, 1988.

(2) Hühnerfuss, H.; et al. *J. Geophys. Res.* **1994**, *99*, 9835.

(3) Mannheimer, R. J.; Schechter, R. S. *J. Colloid Interface Sci.* **1970**, *32*, 195.

(4) Edwards, D. A.; Brenner, H.; Wasan, D. T. *Interfacial Transport Processes and Rheology*; Butterworth-Heinemann: Boston, MA, 1991.

(5) Goodrich, F. C.; Chatterjee, A. K. *J. Colloid Interface Sci.* **1970**, *34*, 36.

(6) Shail, R. *J. Eng. Math.* **1978**, *12*, 59.

(7) Oh, S. G.; Slattery, J. C. *J. Colloid Interface Sci.* **1978**, *67*, 516. Krägel, J.; et al. *Colloids Surf.* **A 1995**, *91*, 169.

(8) Shail, R.; Gooden, D. K. *Int. J. Multiphase Flow* **1981**, *7*, 245.

(9) Brown, A. G.; Thuman, W. C.; McBain, J. W. *J. Colloid Sci.* **1953**, *8*, 491.

(10) Davies, J. T. In *Proceedings of the 2nd International Congress on Surface Activity I*; Butterworths: London, 1957; p 220.

(11) Goodrich, F. C.; Allen, L. H. *J. Colloid Interface Sci.* **1972**, *40*, 329.

(12) Goodrich, F. C.; Allen, L. H.; Poskanzer, A. *J. Colloid Interface Sci.* **1975**, *52*, 201.

(13) Poskanzer, A. M.; Goodrich, F. C. *J. Phys. Chem.* **1975**, *79*, 2122.

(14) Hühnerfuss, H. *J. Colloid Interface Sci.* **1985**, *107*, 84.

(15) Sacchetti, M.; Yu, H.; Zograf, G. *Rev. Sci. Instrum.* **1993**, *64*, 1941.

(16) Kralchevsky, P. A.; Paunov, V. N.; Denkov, N. D.; Nagayama, K. *J. Colloid Interface Sci.* **1994**, *167*, 47.

(17) Velev, O. D.; Denkov, N. D.; Paunov, V. N.; Kralchevsky, P. A.; Nagayama, K. *J. Colloid Interface Sci.* **1994**, *167*, 66.

(18) Petkov, J. T.; Denkov, N. D.; Danov, K. D.; Velev, O. D.; Aust, R.; Durst, F. *J. Colloid Interface Sci.* **1995**, *172*, 174.

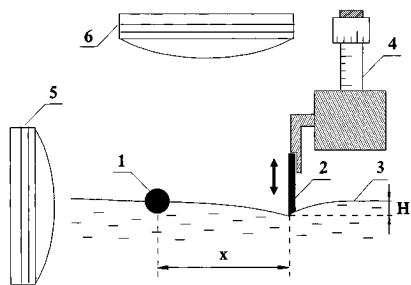


Figure 1. Experimental setup for determination of the drag coefficient of a particle attached to a fluid interface: (1) spherical particle; (2) movable PTFE plate; (3) fluid interface; (4) micrometric screw; (5) horizontal long-focus microscope; (6) vertical long-focus microscope.

$$F = -\pi\gamma[-2qQ_2^2K_1(2qx) + 2Q_2qHe^{-qx} + q(r_2qHe^{-qx})^2] \quad (1)$$

where $Q_2 = r_2 \sin \psi_2$ is the so-called¹⁶ "capillary charge" of the floating particle, r_2 is the radius of the three-phase contact line at the particle surface, and ψ_2 is the meniscus slope angle at this contact line (see Figure 2). $K_1(2qx)$ is a modified Bessel function of the first order, H is the depth of immersion of the vertical hydrophobic plate (that creates the meniscus deformation) with respect to the horizontal plane $z = 0$, x is the distance between the particle center and the plate surface (see Figure 1), q^{-1} denotes the capillary length which characterizes the range of the capillary interaction and is defined as

$$q^2 = \Delta\rho g/\gamma; \quad \Delta\rho = \rho_I - \rho_{II} \quad (2)$$

where γ is the interfacial tension, ρ_I and ρ_{II} are the mass densities of the two fluid phases, and g is the acceleration due to gravity. Thus, for a pure water–air interface ($\Delta\rho = 1 \text{ g/cm}^3$, $\gamma = 72 \text{ mN/m}$) one has $q^{-1} = 2.7 \text{ mm}$.

Equation 1 implies that the force exerted on the particle strongly depends on the particle–wall separation. Therefore, contrary to the known Stokes method for measuring the bulk viscosity of liquids, the particle velocity is not constant throughout our measurements. In order to calculate the particle trajectory, one has to solve the equation of motion of the particle

$$m\ddot{x} = F - \beta\dot{x} \quad (3)$$

where β is the particle drag coefficient and F is given by eq 1. For low Reynolds number the drag force is proportional to the particle velocity \dot{x} and can be expressed as

$$F_d = -\beta\dot{x} = -f_d\beta_s\dot{x} \quad (4)$$

where $\beta_s = 6\pi\eta R_2$ is the Stokes drag coefficient for a sphere immersed in an unbounded fluid of bulk shear viscosity η and f_d denotes the dimensionless drag coefficient for a particle floating on the interface. The final form of the equation of motion becomes

$$\ddot{x} = \frac{F}{m} - f_d \frac{\beta_s}{m} \dot{x} \quad (5)$$

This equation can be solved numerically giving the law of motion of the particle, $x(t)$ and $V(t) = \dot{x}(t)$. The value of f_d is treated as an adjustable parameter. To determine f_d we compare the experimentally measured dependence of the particle–wall separation, x , vs time, t , with the respective theoretical function calculated by means of numerical integration of eq 5 along with eq 1. After

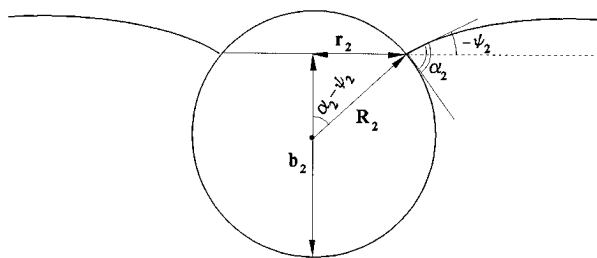


Figure 2. Sketch of a spherical particle attached to a fluid interface. R_2 is the particle radius and α_2 is the three-phase contact angle.

obtaining the surface drag coefficients, f_d , we determine the shear surface viscosity of the surfactant monolayer by means of the theory developed elsewhere.¹⁹ In that paper the low Reynolds number hydrodynamic equations were numerically solved with a nonslip boundary condition at the particle surface and free (in the absence of surfactant monolayer) or viscous (in the presence of monolayer) fluid surface. The viscous coupling between the monolayer and water flows was explicitly taken into account. Both contributions into the drag force (due to the friction within the monolayer and to the dissipation in the subphase) were considered.

The experimental setup is shown in Figure 1. The surfactant solution is poured into the experimental cell and several suction of the surface layer are performed by a clean pipet, connected to a water vacuum pump, to remove traces of surface contaminants. The spherical particle whose surface drag coefficient is to be measured is initially placed at a certain distance from the plate. The latter is made of poly(tetrafluorethylene) (PTFE) and has a sharp lower edge where the three-phase contact line air–water–PTFE is properly fixed. A micrometric screw table is used to vary and to measure the depth of immersion, H . After several minutes, necessary for establishment of equilibrium surfactant adsorption, the first run is performed. The particle is set in motion by a fast change in the vertical position of the plate, which brings about a deformation of the air–water interface. Owing to the lateral capillary force caused by the interfacial deformation, the particle starts to move toward the PTFE wall. Between each two consecutive runs 1 min is allowed for re-establishment of the equilibrium adsorption. Independent measurements by the Wilhelmy plate method and literature data²⁰ confirm that the equilibrium surface tension and adsorption are established within a second at the studied surfactant concentrations. The motion of the particle can be observed through a vertical microscope and recorded by using a CCD camera and video recorder. The records are afterward processed frame by frame using a data image analyzer in order to obtain the particle trajectory $x(t)$. To repeat the experiment, the particle is repelled again at a certain distance from the plate by moving the plate upward (thus changing the shape of the air–water interface from convex to concave). In each experiment we perform at least ten consecutive runs at different depths of immersion H . A horizontal microscope allows one to measure the three-phase contact angle at the particle surface (see Figure 2; for details about the procedure of determination of r_2 , α_2 , and ψ_2 , see ref 16).

In the experiments we used small ($\sim 0.5 \text{ mm}$ in diameter) hydrophobized glass spheres. As a hydrophobizing re-

(19) Danov, K. D.; Aust, R.; Durst, F.; Lange, U. *J. Colloid Interface Sci.* **1995**, *175*, 36.

(20) Sasaki, M.; Yasunaga, T.; Tatsumoto, N. *Bull. Chem. Soc. Jpn.* **1977**, *50*, 858.

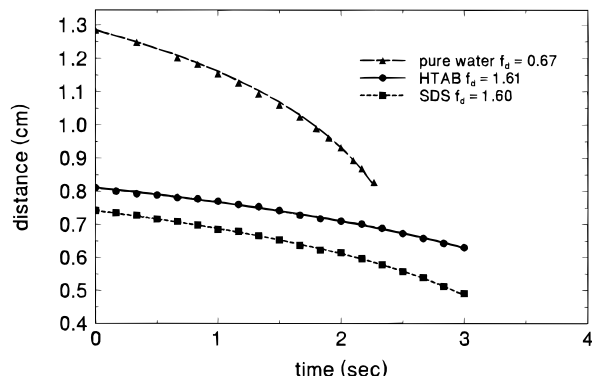


Figure 3. Trajectories of small hydrophobized glass particles floating on a water surface in the absence or in the presence of adsorbed surfactant layers of SDS or HTAB, respectively. The symbols represent the experimental data, while the curves correspond to the numerical solution of the equation of the particle motion.

agent the compound 1,1,1,3,3,3-hexamethyldisilazane (Sigma, St. Louis, MO) was applied. High-purity water obtained from a Milli-Q Organex system (Millipore) was used throughout. Before each experiment the PTFE plate, the glass cell, and the instrumental glassware were cleaned by immersion into hot chromic acid (leaving them inside for not less than 24 h), followed by abundant rinsing with water. The surfactants sodium dodecyl sulfate (SDS) and hexadecyltrimethylammonium bromide (HTAB), products of Sigma, were used to form adsorption monolayers on the air–water interface. The surfactant concentration was 5 times the critical micelle concentration (cmc).^{21,22} This concentration was chosen to avoid the possible influence of the monolayer Gibbs elasticity⁴ on the particle motion.

In Figure 3 the trajectories of particles floating at a pure air–water interface¹⁸ and in the presence of SDS and HTAB monolayers are shown. The curves present the numerical solution of the equation of motion of the respective particle, while the symbols are the experimental data. (For clarity, only the data from one arbitrarily chosen experimental run for each system is shown.) As seen, the agreement between the theory and the experiment is excellent. The smaller slope of the curves $x(t)$ in the presence of surfactants, as compared with the upper curve for pure water, reflects the lowering of the particle velocity due to the friction within the adsorption layer. Correspondingly, the values of the dimensionless surface drag coefficients, f_d , are larger in the presence of surfactants. This is illustrated in Figure 4 where the velocities of the particles in the same experiments are plotted as functions of the capillary force calculated from eq 1. As seen from the figure, the particle velocity is about two times lower (at the same force) in the presence of surfactants compared to the experiment at the pure air–water interface. The linear relationship between the capillary force and the particle velocity means that the inertial term in eq 3 is negligible. The inset in Figure 4 shows the comparison between the experimentally measured (the symbols) and the theoretically calculated (the curves) particle velocities vs time. Again, the agreement is very good.

The average values of the dimensionless surface drag coefficients, determined from a series of experimental runs, are given in Table 1. For comparison, the theoretically calculated values for the drag coefficients at a pure water surface are given in parentheses. As seen from the table

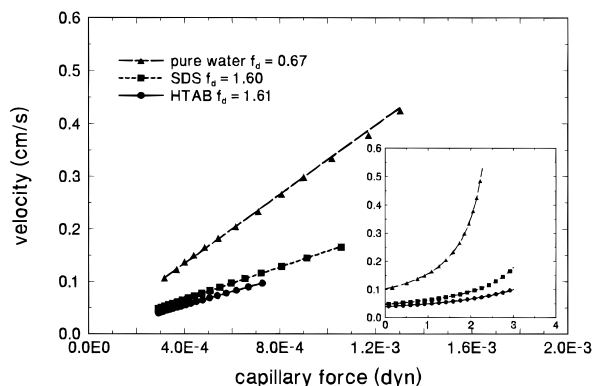


Figure 4. Velocities of small hydrophobized glass particles floating on a water surface (cf. Figure 3) plotted as functions of the capillary force. Symbols represent the experimentally measured velocities and the curves are the numerical solutions of the particle equation of motion. As an inset the velocities (cm/s) as functions of time (s) are shown.

the measured (0.66 ± 0.03) and the calculated (0.66) values of f_d for a pure interface coincide. The contribution of the surfactant adsorption layers to the friction exerted on the particle leads to a substantial increase of the drag coefficient. To calculate the value of the shear surface viscosity, η_s , we applied the theory developed in ref 18. In the latter study the particle drag coefficient is calculated as a function of (i) the three-phase contact angle at the particle surface, α_2 , (ii) the shear surface viscosity, η_s , and (iii) the dilatational surface viscosity, η_d . In our calculations we used for α_2 the values measured microscopically. As shown by Kao *et al.*²³ the magnitude of the dilatational viscosity of low molecular surfactants (SDS and octanoic acid) is around and below 10^{-8} Pa m s. The numerical calculations showed that such small values of η_d do not affect the surface drag coefficient within the limits of the experimental accuracy. Therefore, we determined the values of η_s , shown in Table 1, by comparing the measured surface drag coefficients with the theoretical ones calculated at negligible contribution of η_d . One should note, that the values of the measured drag coefficient (and of the calculated surface viscosity, respectively) did not depend on the applied capillary force and on the particle velocity in a given set of runs. This experimental fact means that the studied surfactant monolayers exhibit Newtonian behavior (i.e., linear force–velocity relationship) at these experimental conditions.

In Table 1 we also show the value of the shear surface viscosity of SDS measured by the sensitive rotating wall knife-edge viscometer.¹³ The comparison (1.45×10^{-6} Pa m s vs 2.3×10^{-6} Pa m s) shows a relatively good agreement in view of the fact that these values are determined by means of rather different experimental methods. This leads us to believe that the measured value of the shear surface viscosity is reliable.

We did not find any data in the literature about the shear surface viscosity of HTAB measured by the sensitive rotating wall knife-edge viscometer. In ref 24 the surface viscosity of an HTAB monolayer was determined by using the canal method.²⁵ The obtained value $\eta_s = 4.5 \times 10^{-5}$ Pa m s²⁴ is 1 order of magnitude larger than the value determined by us (2.04×10^{-6} Pa m s). This difference is most probably due to the shortcomings of the canal method discussed in the literature (see, e.g., refs 13 and

(23) Kao, R. L.; Edwards, D. A.; Wasan, D. T. *J. Colloid Interface Sci.* **1992**, *148*, 247.

(24) Hühnerfuss, H. *J. Colloid Interface Sci.* **1988**, *126*, 384.

(25) Dervichian, D. G.; Joly, M. *J. Phys. Radium* **1939**, *10*, 375.

(21) Lindman, B.; Wenerström, H. *Top. Current Chem.* **1980**, *87*, 1.

(22) Czerniawski, W. *Rocz. Chem.* **1966**, *40*, 1935.

Table 1. Radii and Three-Phase Contact Angles of the Glass Particles Used in Our Experiments and Dimensionless Surface Drag Coefficients and Shear Surface Viscosities Determined Experimentally and Found in the Literature

system	R_2 (cm)	α_2 (deg)	f_d	η_s (Pa m s)	η_s (Pa m s), lit.
pure water–air	0.0222	53	0.66 ± 0.03 (0.66)		
5 × cmc SDS solution–air	0.0216	52	1.57 ± 0.04 (0.66)	$(1.45 \pm 0.03) \times 10^{-6}$	2.3×10^{-6} , ref 13
5 × cmc HTAB solution–air	0.0259	43	1.58 ± 0.03 (0.69)	$(2.04 \pm 0.03) \times 10^{-6}$	4.5×10^{-5} , ref 23

14). As pointed out by Ewers and Sack^{26,27} this method is particularly inaccurate for adsorbed layers of soluble surfactants, because an application of surface pressure would cause part of the layer to dissolve instead of passing through the canal.

In conclusion, our method possesses several advantages in comparison with the existing techniques for measuring the shear surface viscosity. It is relatively simple, without the necessity of a complex equipment. Its sensitivity is rather high, around 3×10^{-8} Pa m s, which makes it especially suitable for experiments with adsorbed or spread monolayers of low-molecular surfactants. It can be applied to a variety of systems of interest (e.g., lipid or protein monolayers) and could be further extended to measurements of the viscosity of lipid bilayers or the interfacial shear viscosity at the boundary between two

liquid phases (e.g., at an oil–water interface). Of substantial interest could be the comparative study of the shear viscosity of lipid monolayers or bilayers in different phase states. However, one should take care that the presence of the sphere could perturb the structure of the lipid layer if the experiment is performed at conditions close to the phase-transition boundary. The capillary forces of controlled magnitude, used in our measurements, could be utilized in other experimental methods as well.

Acknowledgment. This work was supported by the Volkswagen Foundation. We are indebted to Professor I. Ivanov, Professor P. Kralchevsky, and Dr. H. Raszillier for the fruitful discussions. We are also grateful to Dr. Orlin Velev for his valuable help in the experimental setup construction.

LA960007N

(26) Ewers, W. E.; Sack, R. A. *Aust. J. Chem.* **1954**, 7, 40.

(27) Joly, M. In *Recent Progress in Surface Science*; Academic Press: New York, 1964; Vol. 1, p 7.